PHYSICAL REVIEW C VOLUME 36, NUMBER 6 DECEMBER 1987

Angular momentum dependence of complex fragment emission

L. G. Sobotka, D. G. Sarantites, Ze Li, and E. L. Dines
Department of Chemistry, Washington University, St. Louis, Missouri 63130

M. L. Halbert, D. C. Hensley, and J. C. Lisle*
Oak Ridge National Laboratory, Oak Ridge, Tennessee 37830

R. P. Schmitt, Z. Majka,† and G. Nebbia‡
Texas A and M University, College Station, Texas 77843

H. C. Griffin
University of Michigan, Ann Arbor, Michigan 48109

A. J. Sierk
Theoretical Division, Los Alamos National Laboratory, Los Alamos, New Mexico 87545
(Received 8 September 1987)

The angular momentum dependence of large fragment production in long lived reactions is studied by measurements of fragment cross sections from reactions with substantially different angular momentum distributions and the coincident γ-ray multiplicity distributions. The results indicate that the primary l-wave distributions move to larger mean values and decrease in width and skewness with increasing mass symmetry in the decay channel. The results also confirm that the partition of angular momentum in kinetic energy relaxed heavy-ion reactions is that expected for a rigidly rotating intermediate.

One of the fundamental difficulties in the interpretation of heavy-ion reaction data is the large range of angular momenta involved. This inevitably leads to questions concerning how the possible or observed exit channels are distributed within the angular momentum window. An example of this is the study of the tangential component of the frictional force utilizing the transfer of angular momentum from relative motion into intrinsic spin. Such studies often involve comparing reaction times to the times required to reach the equilibrium rigidly rotating condition. Although rigid rotation provides a clear signature in the mass asymmetry dependence of the magnitude of the transferred spin for a fixed or narrow initial l-wave distribution,[1,2] this signature is obscured by a mass asymmetry fractionation of a wide initial l-wave distribution.[3,4]

In this work we investigate the l-wave distributions which contribute to different exit channel charge asymmetries in long lived reactions. (We do not distinguish between statistical decay of a completely fused compound nucleus and long lived deep inelastic reactions. We will, however, compare experimental results to equilibrium calculations for reasons which will be mentioned later.) Two experimental techniques are used in this study. First, fragment cross sections from two reactions with substantially different angular momentum windows are compared. Second, complete γ-ray multiplicity (M_γ) distributions are obtained as a function of charge asymmetry for one of these reactions. This last feature is an important improvement over previous studies which, at best, determined reliably only the first and, on occasion, the second moments[5,6] of the M_γ distributions.

The two systems compared in this work are 782 MeV ^{93}Nb+^{9}Be and 200 MeV ^{45}Sc+^{65}Cu. The experimental results for the ^{93}Nb+^{9}Be system have been previously published.[7] The new experimental data reported here involve the ^{45}Sc+^{65}Cu system. Self-supporting ^{65}Cu target foils (enriched to 99.7% in the mass 65 isotope and 320–450 μg/cm^2 thick) were bombarded with a 200 MeV ^{45}Sc beams from the Holifield Heavy-Ion Research Facility. In this experiment the intermediate mass fragments were detected by two large solid angle telescopes with ion chambers as the ΔE detectors and Si(Li) as the E detectors. Each Si(Li) detector consisted of four strips (1.1 cm×4.6 cm) that were position sensitive in the long direction. The telescopes subtended 18° in the laboratory system, and each was centered at 40° and 55° from the beam direction at different times during the experiment.

The spin spectrometer[8] served as the γ-ray detector and measured simultaneously M_γ, the total γ-ray deexcitation energy and the γ-ray angular correlations. In this experiment 70 of the 72 detectors were used, covering 94.5% of 4π sr. The data were processed to distinguish γ rays from neutron pulses (utilizing time-of-flight information) and to unfold the total γ-ray pulse height versus number of γ-ray hits (k) to yield total E_γ vs M_γ (see Ref. 8 for the details of these procedures).

Table I lists several quantities that are useful for comparing these systems. The completely fused systems have atomic numbers of $A=102$ and 110 with similar excitation energies (see below) but vastly different values for the critical angular momentum for fusion, $l_{\text{crit.}}$ In both cases the bulk of the reaction cross section is expected to fuse. In order to bias against the smaller nonequilibrated components, the data discussed here are those collected near

TABLE I. Quantities characterizing the reactions of interest.

System	E_{lab} (MeV)	CN	E^* (MeV)	l_{crit}[a] ($\hbar$)	l_m[b]	x[c]	y[d]
$^{93}Nb+^{9}Be$	782	^{102}Rh	78	34	43	0.40	0.05
$^{45}Sc+^{65}Cu$	200	^{110}Sn	94	70	80	0.45	0.17

[a]The critical angular momentum for fusion given by the Bass model (Ref. 12).
[b]The maximum angular momentum for a grazing collision.
[c]$x = Z^2/50A$.
[d]$y = 2l^2_{crit}/A^{7/3}$.

$\theta_{C.M.} \sim 90°$, which is far behind the classical grazing angles (25° behind for the $^{45}Sc+^{65}Cu$ system). Due to the above arguments, as well as the inherent simplicity, we will compare these data to equilibrium calculations. However, for present purposes, we believe that it is immaterial whether the mechanism is true compound nucleus decay, deep inelastic reaction products, or a mixture of these. In a forthcoming paper in which excitation functions are presented, we deal with the time scale for these reactions.

Large fragment production in the kinetic energy relaxed component of low energy reactions is controlled by the relative energy cost of producing critical decay configurations of different mass asymmetries. These energies, which have been called a ridge line potential,[9] together with a few statistical parameters, will determine the decay probabilities of a compound nucleus. For reactions which are not equilibrated in the mass asymmetry degree of freedom, the ridge potential is still of fundamental importance; however, the reaction time and diffusion rates also play an important role. The inset in Fig. 1 shows the topology of a surface composed of ridge line potentials as a function of angular momentum for the compound system ^{110}Sn. These barriers are calculated with the finite range (FR) corrected rotating-liquid-drop model of Ref. 10, extended to consider the asymmetric conditional saddles. A system restricted to low angular momenta is only sensitive to the region which exhibits a broad region around symmetry of rather large barriers. The corresponding cross sections will reflect this shape with plummeting cross sections with increasing atomic number until the barrier plateau is reached, after which the cross sections will remain constant. On the other hand, a system with angular momenta extending to larger values will respond to generally smaller barriers; thus, larger cross sections will be observed and, if sufficient angular momentum is present, to the stable symmetric saddle. The last feature is the characteristic of heavy element fission and leads to increasing yields as symmetry is approached.

These are exactly the trends observed for the low and high spin systems (Fig. 1). This indicates that the barrier surface has the general topology shown in the inset and that the $^{93}Nb+^{9}Be$ system is restricted to the low spin region while the $^{45}Sc+^{65}Cu$ system is not. A knowledge of heavy-ion and fission reactions makes these results rather transparent and therefore not at all surprising. However,

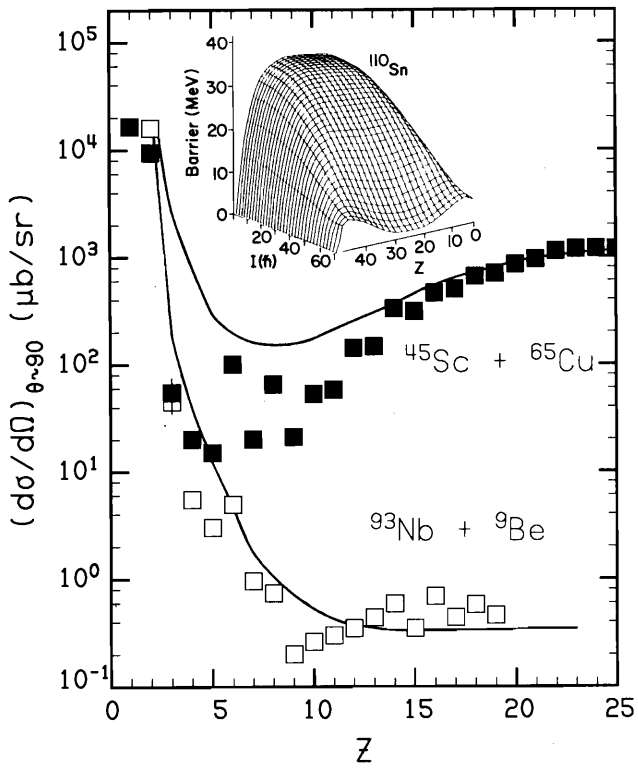

FIG. 1. Measured differential cross sections for the $^{45}Sc+^{65}Cu$ (solid symbols) and $^{93}Nb+^{9}Be$ (open symbols) systems. The solid lines are the result of the equilibrium calculations described in the text. For these calculations, a level density parameter of $a = A/7.1$ was used. The inset is a surface plot of the asymmetry and angular momentum dependent barrier for ^{110}Sn decay calculated with FR corrected rotating liquid drop model.

what is not known is the nature of the l-wave distributions contributing to each decay channel. We now turn our attention to this subject.

As mentioned earlier, the γ-ray data were analyzed to provide M_γ and the total γ-ray energy, as well as the individual γ-ray energies. The experimental M_γ distributions for selected elements from the $^{45}Sc+^{65}Cu$ system are shown in Fig. 2(a). The distributions for the low Z elements are broad with the most probable values being significantly greater than the average values. As the atomic number increases, the M_γ distributions become narrower and more symmetric, with lower mean M_γ values.

In order to relate the M_γ distributions of Fig. 2(a) to transferred spin distributions, we must investigate the distribution of γ-ray multipolarities emitted in the reaction. We have not undertaken a detailed study of this point. We can, however, answer the question of what asymmetry region is consistent[11] with a preponderance of stretched $E2$ transitions. The γ-ray angular distributions in the plane perpendicular to the beam for elements that are more than one charge removed from 8 show the distinctive stretched $E2$ form.[12] The distributions for nitrogen and fluorine indicate an increased proportion of multipolarities other than stretched $E2$ and that for oxygen shows no an-

TABLE I. Quantities characterizing the reactions of interest.

System	E_{lab} (MeV)	CN	E^* (MeV)	l_{crit}[a] ($\hbar$)	l_m[b]	x[c]	y[d]
$^{93}Nb+^{9}Be$	782	^{102}Rh	78	34	43	0.40	0.05
$^{45}Sc+^{65}Cu$	200	^{110}Sn	94	70	80	0.45	0.17

[a]The critical angular momentum for fusion given by the Bass model (Ref. 12).
[b]The maximum angular momentum for a grazing collision.
[c]$x = Z^2/50A$.
[d]$y = 2l^2_{crit}/A^{7/3}$.

$\theta_{C.M.} \sim 90°$, which is far behind the classical grazing angles (25° behind for the $^{45}Sc+^{65}Cu$ system). Due to the above arguments, as well as the inherent simplicity, we will compare these data to equilibrium calculations. However, for present purposes, we believe that it is immaterial whether the mechanism is true compound nucleus decay, deep inelastic reaction products, or a mixture of these. In a forthcoming paper in which excitation functions are presented, we deal with the time scale for these reactions.

Large fragment production in the kinetic energy relaxed component of low energy reactions is controlled by the relative energy cost of producing critical decay configurations of different mass asymmetries. These energies, which have been called a ridge line potential,[9] together with a few statistical parameters, will determine the decay probabilities of a compound nucleus. For reactions which are not equilibrated in the mass asymmetry degree of freedom, the ridge potential is still of fundamental importance; however, the reaction time and diffusion rates also play an important role. The inset in Fig. 1 shows the topology of a surface composed of ridge line potentials as a function of angular momentum for the compound system ^{110}Sn. These barriers are calculated with the finite range (FR) corrected rotating-liquid-drop model of Ref. 10, extended to consider the asymmetric conditional saddles. A system restricted to low angular momenta is only sensitive to the region which exhibits a broad region around symmetry of rather large barriers. The corresponding cross sections will reflect this shape with plummeting cross sections with increasing atomic number until the barrier plateau is reached, after which the cross sections will remain constant. On the other hand, a system with angular momenta extending to larger values will respond to generally smaller barriers; thus, larger cross sections will be observed and, if sufficient angular momentum is present, to the stable symmetric saddle. The last feature is the characteristic of heavy element fission and leads to increasing yields as symmetry is approached.

These are exactly the trends observed for the low and high spin systems (Fig. 1). This indicates that the barrier surface has the general topology shown in the inset and that the $^{93}Nb+^{9}Be$ system is restricted to the low spin region while the $^{45}Sc+^{65}Cu$ system is not. A knowledge of heavy-ion and fission reactions makes these results rather transparent and therefore not at all surprising. However,

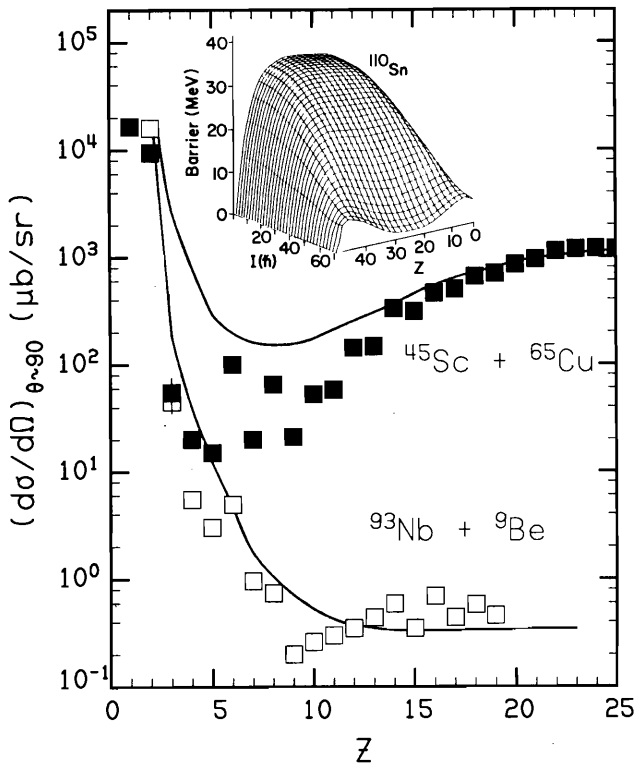

FIG. 1. Measured differential cross sections for the $^{45}Sc+^{65}Cu$ (solid symbols) and $^{93}Nb+^{9}Be$ (open symbols) systems. The solid lines are the result of the equilibrium calculations described in the text. For these calculations, a level density parameter of $a = A/7.1$ was used. The inset is a surface plot of the asymmetry and angular momentum dependent barrier for ^{110}Sn decay calculated with FR corrected rotating liquid drop model.

what is not known is the nature of the l-wave distributions contributing to each decay channel. We now turn our attention to this subject.

As mentioned earlier, the γ-ray data were analyzed to provide M_γ and the total γ-ray energy, as well as the individual γ-ray energies. The experimental M_γ distributions for selected elements from the $^{45}Sc+^{65}Cu$ system are shown in Fig. 2(a). The distributions for the low Z elements are broad with the most probable values being significantly greater than the average values. As the atomic number increases, the M_γ distributions become narrower and more symmetric, with lower mean M_γ values.

In order to relate the M_γ distributions of Fig. 2(a) to transferred spin distributions, we must investigate the distribution of γ-ray multipolarities emitted in the reaction. We have not undertaken a detailed study of this point. We can, however, answer the question of what asymmetry region is consistent[11] with a preponderance of stretched $E2$ transitions. The γ-ray angular distributions in the plane perpendicular to the beam for elements that are more than one charge removed from 8 show the distinctive stretched $E2$ form.[12] The distributions for nitrogen and fluorine indicate an increased proportion of multipolarities other than stretched $E2$ and that for oxygen shows no an-

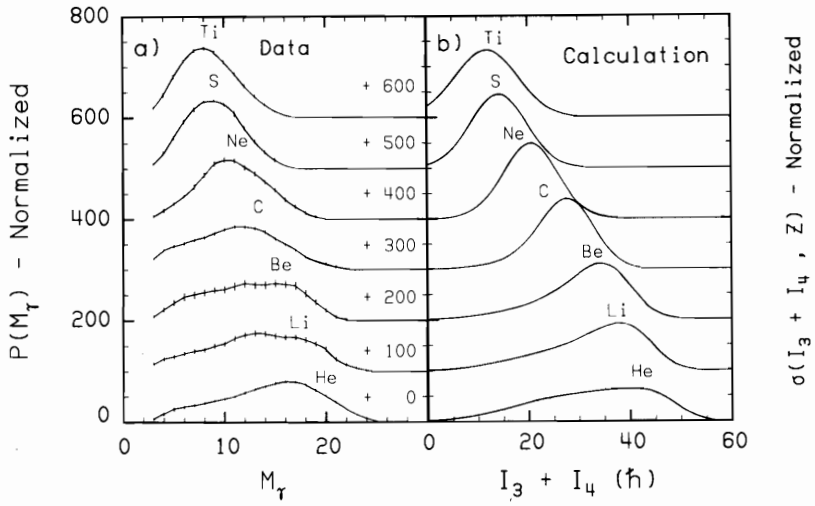

FIG. 2. (a) Experimental γ-ray multiplicity distributions (M_γ) in coincidence with He, Li, Be, C, Ne, S, and Ti fragments. The M_γ distributions have been normalized to 1000. The distributions have been shifted on the ordinate by the values indicated in the figure. (b) Calculated transferred spin distributions for the same elements as (a). The curves are normalized and offset in the same fashion as for (a).

gular dependence at all. This variation of the multipolarities present is undoubtedly due to the influence of the $N=50$ shell in the heavy partner. The complementary fragment to ^{16}O is $^{92}Mo_{50}$ (the most probable sequential decay is $2n$).

The similarity of the γ-ray angular distributions, when the fragment is not close in charge to oxygen, suggests that the functions that convert M_γ to transferred spin, I_3+I_4, should be similar. On the other hand, around $Z=8$, the conversion function may be substantially different.

The discussion above indicates that the transferred angular momentum does in fact decrease as the fragments become more mass-symmetric. This conclusion is reinforced by recalling the conclusion reached from Fig. 1, that the symmetric fragments from the $^{45}Sc+^{65}Cu$ system result from large angular momenta. The trend of a strongly decreasing fraction of the total spin transferred to the fragments is that expected if the partition is frozen at a rigidly rotating configuration. In this case the fraction is determined by the ratio of the moments of inertia, $f=(\mathcal{I}_3+\mathcal{I}_4)/(\mathcal{I}_3+\mathcal{I}_4+\mathcal{I}_{rel})$, where $\mathcal{I}_i$ are the moments of inertia of the two fragments and that for relative motion. This fraction is a minimum at symmetry and approaches 1 in the large asymmetry limit of one fragment with all the mass. This is the argument which has been used previously to argue for a rigidly rotating intermediate in deep inelastic reactions.

The information which has not been available previously is contained in the full distributions shown in Fig. 2. In an effort to understand these distributions, we will use the traditional fission transition state formalism extended to explicitly treat the mass or charge asymmetry coordinate.[7,13] This model has been used in previous complex fragment emission studies at both low[4,14,15] and intermediate[16,17] energies.

The main difference between the present calculations and those reported in previous low energy works is that the mass asymmetry and angular momentum dependent barriers for fragments with $Z>2$ come from a finite range corrected liquid drop model rather than from a sphere-sphere or a spheroid-spheroid model. This improvement removes the distance between centers of the nearest fragments as a free parameter. This variable was adjusted in previous works in order to obtain agreement between the experimental total kinetic energy (TKE) and the sum of the Coulomb and relative rotational energies of the fragments. A minor modification in the model calculation is that multistep emission is now included. Emission from any of the light particle decay products in a $5(Z)\times5(N)$ block of the Segré chart (CN in the upper right corner) is considered.

The calculated primary l-wave distributions contributing to several selected decay channels are shown in Fig. 3. As the decay channel asymmetry decreases, the contributing l-wave distribution moves to larger average values and

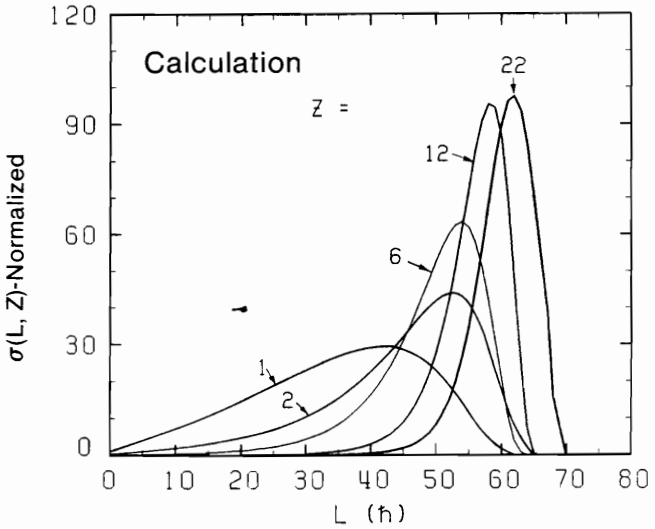

FIG. 3. Calculated initial l-wave distributions for selected exit channels for the $^{45}Sc+^{65}Cu$ system.

becomes narrower. These trends can again be understood by inspecting the inset in Fig. 1. The corresponding cross sections are shown as solid lines in Fig. 1. The agreement is quite good over most of the asymmetry range for both systems. The cross sections for creating symmetric or near symmetric fragments are more than three orders of magnitude higher for the $^{45}Sc+^{65}Cu$ system than for the $^{93}Nb+^{9}Be$ system. This difference is due to the larger angular momenta available in the $^{45}Sc+^{65}Cu$ system. The influence of the excitation energy was studied by running the calculation for the $^{93}Nb+^{9}Be$ system at the excitation energy of the $^{45}Sc+^{65}Cu$ system. This resulted in an increase in the symmetric cross sections by only a factor of 2.

In order to calculate the transferred spin, we assume rigid rotation of two spheres separated by 2 fm. We have also included fluctuations in the transferred spin.[18] The resulting calculated I_3+I_4 distributions are shown in Fig. 2(b). The rigid rotation model inverts the distributions from those in Fig. 3. (High Z values with large mean l values have low mean I_3+I_4 values, while low Z values with low mean l values have high mean I_3+I_4.) On the other hand, the trends in the widths and, to some extent, the skewnesses are preserved. (Low Z products have broad asymmetric distributions while high Z products have narrow, nearly symmetric distributions.)

Comparisons of the experimental distributions, Fig. 2(a), to the calculated ones, Fig. 2(b), indicate that the model does reproduce the main experimental features. The agreement between the trends in the mean values of the calculated (I_3+I_4) and the measured (M_γ) distributions supports the rigid rotation model. The favorable comparison between the calculated and experimental widths and skewnesses does indicate that the forms of the primary l-wave distributions are similar to those shown in Fig. 3 (The larger the fragment, the more symmetric the decay; the narrower is the contributing primary l-wave distribution.) In this regard, we must mention that the inclusion of the fluctuations[18] is essential in order to reproduce the widths of the l-wave distributions near symmetry. This result agrees with the conclusion of the previous works in which widths were reported.[5,6] However, unlike the full distributions shown in Fig. 2, these earlier studies did not reveal any significant trends in the higher moments with charge asymmetry.

In summary, we have shown that the exit channel fragment spin distributions retain information on the primary l-wave distributions contributing to these exit channels. The information is contained in the higher moments of these distributions. The relation between mean values is less direct due to the strong dependence on mass asymmetry of the magnitude of the unobserved exit channel orbital angular momentum.

This work was supported in part by the U.S. Department of Energy under Contracts No. DE-FC02-87ER40316, No. DE-AS02-76ER04052, and No. DE-AC05-84OR21400. One of us (L.G.S.) is pleased to acknowledge support from a U.S. Presidential Young Investigator Award. Oak Ridge National Laboratory is operated by Martin Marietta Energy Systems, Inc.

*Permanent address: Schuster Laboratory, University of Manchester, Manchester M13 9Pl, England.

†Permanent address: Institute of Physics, Jagellonian University, Ul. Reymonta 4, Krakow, Poland.

‡Permanent address: Istituto Nationale di Fisica Nucleare, Sezione di Padova, Italy.

[1]P. Glässel *et al.*, Phys. Rev. Lett. **38**, 331 (1977).

[2]M. N. Namboodiri *et al.*, Phys. Rev. C **20**, 982 (1979).

[3]M. M. Aleonard *et al.*, Phys. Rev. Lett. **40**, 622 (1978).

[4]L. G. Sobotka *et al.*, Nucl. Phys. **A371**, 510 (1981).

[5]P. R. Christensen *et al.*, Nucl. Phys. **A349**, 217 (1980).

[6]R. A. Dayras *et al.*, Phys. Rev. C **22**, 1485 (1980).

[7]L. G. Sobotka *et al.*, Phys. Rev. Lett. **53**, 2004 (1984).

[8]M. Jääskeläinen *et al.*, Nucl. Instrum. Methods **204**, 385 (1983).

[9]L. G. Moretto, Nucl. Phys. **A247**, 211 (1975).

[10]A. J. Sierk, Phys. Rev. C **33**, 2039 (1986).

[11]We use the word consistent because we cannot distinguish between stretched $E2$ and nonstretched ($\Delta I=0$) dipole transitions.

[12]Z. Majka *et al.*, Phys. Rev. Lett. **58**, 322 (1987).

[13]W. J. Swiatecki, Austr. J. Phys. **36**, 641 (1983).

[14]L. G. Sobotka *et al.*, Phys. Rev. Lett. **51**, 2187 (1983).

[15]M. A. McMahan *et al.*, Phys. Rev. Lett. **54**, 1995 (1985).

[16]F. Auger *et al.*, Phys. Rev. C **35**, 190 (1987).

[17]R. J. Charity *et al.*, Phys. Rev. Lett. **56**, 1354 (1986).

[18]R. P. Schmitt and A. J. Pacheco, Nucl. Phys. **A379**, 313 (1982).